Thermochimica Acta, 186 (1991) 69–87
Elsevier Science Publishers B.V., Amsterdam

A phenomenological model for the enthalpy relaxation of glasses. Part 1. A single relaxation time approach for non-crystalline selenium

F.L. Cumbrera [a] and A. Muñoz [b]

[a] *Departamento de Física, Facultad de Ciencias, Universidad de Extremadura, Badajoz (Spain)*
[b] *Departamento de Física de la Materia Condensada e Instituto de Ciencias de los Materiales, Facultad de Física, Sevilla (Spain)*

(Received 12 December 1990)

Abstract

Relaxation phenomena have become a major concern in non-crystalline materials. In the present paper we deal with a phenomenological model, based on the Kovacs equation, describing enthalpic relaxation in glasses. Only a single relaxation time, τ, is considered. The model is built up in steps of progressive complexity. Here, two cases are distinguished: (i) a pure thermal dependence for τ, and (ii) a combined dependence with temperature and the departure from equilibrium. Comparisons with calorimetric measurements performed on amorphous selenium show generally good agreement, but indicate the need for consideration of a distribution of relaxation times.

1. INTRODUCTION

Empirical approaches to describe the phenomena associated with the glass transition are particularly valuable to represent the enthalpy relaxation of a large number of non-crystalline materials [1–4]. Up to now the most satisfying account of structural relaxation in glasses is in terms of the model of Kovacs et al. [5,6].

Conceptually, the KAHR (Kovacs–Aklonis–Hutchinson–Ramos) equations are derived in a general way from the classical order parameter model. In this model it is assumed that the state of the system depends on temperature, T, pressure, P, and a number of order parameters Z_i. Assuming a single ordering parameter Z, the thermodynamic potential $\phi(T, P, Z)$ can be decomposed in an infinitesimal change as follows

$$d\phi = (\partial\phi/\partial T)_{P,Z}\, dT + (\partial\phi/\partial P)_{T,Z}\, dP + (\partial\phi/\partial Z)_{T,P}\, dZ$$

At constant pressure, and adopting the enthalpy H as ϕ, we obtain

$$dH/dt = (\partial H/\partial T)_{P,Z}\, dT/dt + (\partial H/\partial Z)_{T,P}\, dZ/dt$$

where t is the experimental time.

0040-6031/91/$03.50

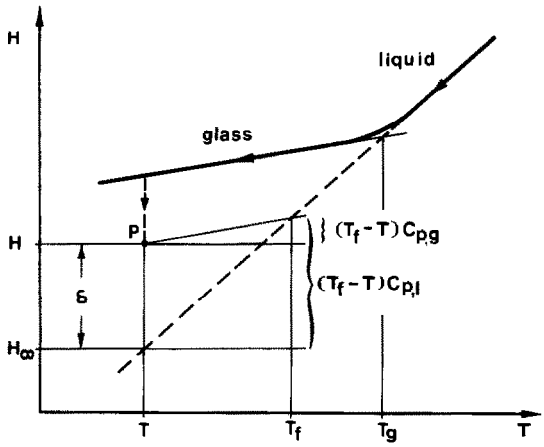

Fig. 1. Temperature dependence of the enthalpy H in the formation process of a glass and isothermal evolution at temperature T.

Accordingly, the heat capacity at constant pressure of the glass and the supercooled liquid can be expressed as

$$C_{p,g} = (\partial H/\partial T)_{P,Z}$$

$$C_{p,l} = (\partial H_\infty/\partial T)_{P,Z}$$

where H_∞ is the equilibrium enthalpy at temperature T.

Defining a new variable, $\delta = H - H_\infty$, which is a measure of the departure from equilibrium, and assuming that a variation of the ordering parameters will produce a change δ, the rate of which is assumed to be proportional to the instantaneous departure from equilibrium, it is straightforward to obtain the single Kovacs equation

$$-\mathrm{d}\delta/\mathrm{d}t = \Delta C_p q + \delta/\tau$$

where $\Delta C_p = C_{p,l} - C_{p,g}$ is the increment of the heat capacity in the transition range, τ is the relaxation time and $q = \mathrm{d}T/\mathrm{d}t$ is the cooling or heating rate. Figure 1 displays the most relevant magnitudes considered in the text.

In the frame of an N ordering parameters theory, Kovacs et al. decomposed δ into N finite portions such that

$$\delta = \sum_{i=1}^{N} \delta_i$$

in which each δ_i indicates a fractional departure from equilibrium.

Physically, the order parameters might represent either molecular motions controlling a specific fraction δ_i of the whole δ or such things as the number of broken bonds of various types, the number of sites with a particular

geometry, etc. We can assume in any case that each δ_i yields the corresponding Kovacs equation, leading to a system of N differential equations

$$-\mathrm{d}\delta_i/\mathrm{d}t = \Delta C_{p_i} q + \delta_i/\tau_i \qquad (i = 1, \ldots N)$$

which are denominated the KAHR equations.

In previous papers [7,8] we have reported some enthalpic relaxation phenomena through the glass transition region in thermally evaporated amorphous specimens of Se and $Se_{100-x}Bi_x$ ($x \leqslant 3.4$). Details of the experimental arrangement used were described previously [7,8]. Nevertheless, it is interesting to point out that specific heat measurements were made with a Perkin–Elmer DSC-II-C differential scanning calorimeter and the rejuvenation method [9] for the heat treatments was used in order to achieve the best repeatability of the measurements. From the performed experiments these phenomena were classified in a qualitative fashion as: (i) cooling rate effects, (ii) aging effects and (iii) memory effects. Some of the results were interpreted on the basis of the activation energy spectra (AES). This last formalism allowed us to formulate an alternative description of the structural relaxation.

The aim of the present work is to develop a model, in the frame of a distribution of relaxation times, which accounts for the main features of structural relaxation of amorphous selenium. In fact, the occurrence of memory effects observed after two successive temperature steps (crossover phenomena) or more such steps involves a multiplicity of relaxation mechanisms controlling the structural relaxation. Although in recent years different approaches to this problem have been proposed [2,5,6,10–12], its application was based mainly on the simpler and mathematically convenient temperature dependence for τ suggested by Twyman [13]. In this paper we have assumed the Narayanaswamy dependence [14], which is a more general view and is consistent with an Arrhenius dependence.

We shall build up our model gradually, following three consecutive steps. The present paper deals with the simple approximation of a single relaxation time, τ. Here, two cases may be distinguished: (i) a pure thermal dependence for τ, $\tau = \tau(T)$, or (ii) a combined dependence with temperature and structure, $\tau = \tau(T, \delta)$. In applying these approaches, only limited success was achieved, suggesting the need for the more general approach adopted in a forthcoming paper: a third step considering the case of a distribution of relaxation times. However, we adopt a continuous integral representation of δ instead of the discrete representation of the Kovacs model. This approach, suggested by Chow and Prest [15], appears as a logical extension of the discrete model when N is large.

The numerical calculations are fitted to calorimetric experimental data for evaporated amorphous selenium and compared with the results deduced by the alternative AES method. Both approaches give us a picture of the dominant process in the relaxation of amorphous selenium. We have not

attempted to fit the more complex Se–Bi experimental results, where compositional changes (spinodal transformation) add to structural relaxation.

2. SEPARATION OF THERMAL AND STRUCTURAL CONTRIBUTIONS TO τ

Tool [16] was the first to propose that one can separate the relative contributions of structural parameters, here characterized by δ, from that of temperature by means of an adjustable partition parameter.

In practice, the separation is as follows:

$$\ln \tau = \ln A + f(T) + g(\delta)$$

where $f(T)$ is the pure thermal dependence and $g(\delta)$ characterizes the structural state.

So far the expression

$$g(\delta) = -c(H - H_\infty)$$

has been used extensively (where c is a constant). Alternatively, the concept of fictive temperature, T_f, describes the deviation of a system from equilibrium for any freezing-in transition [10,16]. The fictive temperature is the actual temperature at which the configuration would be at equilibrium. For an experiment of enthalpic relaxation, T_f may be obtained at the intersection of the extrapolation of the equilibrium line with the straight line through P (the point representing the actual configuration) and whose slope is $C_{p,g}$. In this way, $g(\delta)$ may be expressed as

$$g(\delta) = -(T_f - T)$$

which is equivalent to the former expression because of the relation

$$H - H_\infty = \Delta C_p (T_f - T)$$

which is realized if the heat capacities, $C_{p,l}$ and $C_{p,g}$, both remain constant in the thermal region studied (Fig. 1).

With respect to the thermal dependence, $f(T)$, for practical reasons many authors have adopted the linear law

$$f(T) = -bT$$

Nevertheless, in our work the Arrhenius dependence, which contains the activation energy, E

$$f(T) = E/kT$$

has been used. This relation is included in the Narayanaswamy form for τ used throughout this paper:

$$\tau(T, \delta) = A \exp(xE/kT) \exp[(1 - x)E/kT_f]$$

in which x is a partition parameter ($0 < x \leqslant 1$) characterizing the pure contribution of temperature to τ. The Narayanaswamy form for τ is

consistent with a viscosity which obeys an Arrhenius law within and above the glass transition range.

The alternative form

$$\tau(T, \delta) = A \exp(-BT) \exp[-(1-x)B(T_f - T)]$$

was analyzed by Hutchinson and Kovacs [17].

The treatment which follows in the next section concerns the case of pure thermal dependence ($x = 1$), $\tau = \tau(T)$.

3. PURE THERMAL DEPENDENCE

3.1 Cooling equations

Here we consider the isobaric cooling ($q^- < 0$), assuming the cooling rate to remain constant during the experiment. One can write $T - T_0 = q^- t$, where T_0 is the starting temperature.

Hence, the relaxation time is

$$\tau = \tau_0 \exp(E/kT) = \tau_0 e^x$$

with $x = E/kT$.

Differentiating this last expression we obtain

$$dx = -mx^2 \, dT$$

where $m = k/E$

In this way, the single Kovacs equation can be written in the form

$$d\delta/dx + \delta \frac{b}{x^2 e^x} = a/x^2$$

by the substitutions

$$a = \Delta C_p/m > 0$$

$$b = \frac{-1}{q^- \tau_0 m} > 0$$

In this last equation the preexponential factor τ_0, together with E and ΔC_p, are considered material constants, whereas q and the pair of starting conditions (T_0, δ_0) are experimental conditions. The integration of the equation depends critically on the sign of q; this is the reason we analyze separately the cooling and heating experiments.

For the cooling equation the value of δ for any temperature is

$$\delta(x) = F(x) e^{u(x)} + \delta_0 e^{u(x)-u_0}$$

where $u(x) = b\left[\frac{1}{x e^x} + R(x)\right]$

with $R(x) = \int_{x_0}^{x} t^{-1} \, e^{-t} \, dt$, $F(x) = a \int_{x_0}^{x} t^{-2} \, e^{-u(t)} \, dt$

and $x_0 = E/kT_0$.

In practice, the cooling experiment starts from an equilibrium state ($\delta_0 = 0$). Then the solution for δ may be written as

$$\delta(x) = a \int_{x_0}^{x} \alpha^{-2} \exp[u(x) - u(\alpha)] \, d\alpha$$

and the argument of the exponential is given by

$$u(x) - u(\alpha) = b\left\{\left(\frac{1}{x \, e^{x}} - \frac{1}{\alpha \, e^{\alpha}}\right) + [E_1(\alpha) - E_1(x)]\right\}$$

$E_1(x)$ being the exponential integral function

$$E_1(x) = \int_{x}^{\infty} t^{-1} \, e^{-t} \, dt$$

For practical cases, the numerical computation of $E_1(\alpha) - E_1(x)$ necessitates working in quadruple precision in order to get sufficiently accurate numbers.

Now, it can be shown that a simple relationship exists between the experimentally available glass transition temperature, T_g, and the material constant E. It has long been appreciated that when a glass-forming system is frozen its fictive temperature is constant (isoconfigurational state). In this sense the glass temperature is

$$T_g = \lim_{T \to 0} (T_f - T)$$

but for continuous cooling T_f is represented by

$$T_f = \delta / \Delta C_p + T$$

Thus,

$$T_g = \lim_{T \to 0} \frac{E}{k} \int_{x_0}^{x} \alpha^{-2} \exp[u(x) - u(\alpha)] \, d\alpha$$

$$= (E/k) \int_{x_0}^{\infty} \alpha^{-2} \exp\{-b[e^{-\alpha}/\alpha - E_1(\alpha)]\} \, d\alpha$$

On the other hand, the $E_1(\alpha)$ function can be written [18]

$$E_1(\alpha) = e^{-\alpha}/\alpha[1 - 1!/\alpha + 2!/\alpha^2 \ldots] = e^{-\alpha}/\alpha[1 - \Delta(\alpha)]$$

where the $\Delta(\alpha)$ function

$$\Delta(\alpha) = \sum_{n=1}^{\infty} (-1)^{n-1} n!/\alpha^n$$

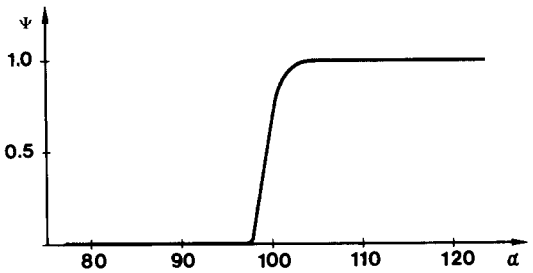

Fig. 2. Plot of $\psi(\alpha)$ versus α for $b = 10^{47}$.

is an alternate series which rapidly converges toward zero as α increases. Hence

$$T_g = (E/k)\int_{x_0}^{\infty} \alpha^{-2} \exp\left[\frac{-b\,\Delta(\alpha)}{\alpha\, e^{\alpha}}\right] d\alpha$$

The function $\psi(\alpha) = \exp[-b\,\Delta(\alpha)\alpha^{-1}\, e^{-\alpha}]$ has some pleasing features arising from the properties of the $\Delta(\alpha)$ function and from the large values of parameter b (for a practical case $b \simeq 10^{47}$). In fact $\psi(\alpha)$ behaves like a step function; for some $\bar{\alpha}$ value

$$\psi(\alpha) \simeq 0, \quad \alpha < \bar{\alpha}$$

$$\psi(\alpha) \simeq 1, \quad \alpha > \bar{\alpha}$$

as one can see in Fig. 2. The value $\bar{\alpha}$ should correspond approximately to the inflexion point of $\psi(\alpha)$ located at its sharp rise. In deriving the value of $\bar{\alpha}$ we have shown the straightforward relationship

$$\Delta'(\alpha) = \Delta(\alpha)(1 + 1/\alpha) - 1/\alpha$$

from which we obtain

$$\bar{\alpha}\, e^{\bar{\alpha}}(\bar{\alpha} - 2) = b$$

which may be simplified to the expression

$$\bar{\alpha}^2\, e^{\bar{\alpha}} = b$$

since in practice $\bar{\alpha} \simeq 10^2$.

In this way we have

$$T_g = E/k\int_{\bar{\alpha}}^{\infty} \frac{d\alpha}{\alpha^2} = \frac{E}{k\bar{\alpha}}$$

The above relation shows that, for any practical case, the activation energy, E, is the relevant parameter controlling the correct position of T_g. For purposes of discussion we shall now consider the crude approximation

$$e^{\bar{\alpha}} = b$$

instead of the full transcendental equation providing $\bar{\alpha}$ (in fact, the error in

obtaining $\bar{\alpha}$ by means of this approximation is smaller than 9%). Then we can express T_g as

$$T_g = \frac{E}{k \ln \dfrac{1}{\tau_0 \mid q^- \mid m}}$$

and differentiating with respect to $\mid q^- \mid$ one obtains the expression

$$\mathrm{d}T_g/\mathrm{d} \ln \mid q^- \mid = \frac{kT_g^2}{E}$$

showing that the variation of $T_g(\mid q^- \mid)$ with the cooling rate is also controlled by E. This result agrees with the results of Moynihan et al. [19] and Kovacs et al. [6] derived from different expressions for the relaxation time.

Moreover, the following equivalent relationship

$$\frac{\mathrm{d} \ln \mid q^- \mid}{\mathrm{d}(1/T_g)} = -E/k$$

suggests a powerful way for deriving the activation energy from the $T_g(q^-)$ dependence.

Finally, it must be said that for an isothermal annealing stage ($q = 0$) the Kovacs equation leads to

$$\delta = \delta_0 \, \mathrm{e}^{-t/\tau}$$

in which τ is a constant, being a constant temperature T.

3.2 Heating equations

In this case we have $q^+ > 0$; we perform the same substitutions as for the cooling case except

$$b = \frac{1}{mq^+\tau_0} > 0$$

and we obtain the heating equation

$$\mathrm{d}\delta/\mathrm{d}x + \delta\left(-\frac{b}{x^2 \, \mathrm{e}^x}\right) = a/x^2$$

In this way the solution is

$$\delta(x) = G(x) \, \mathrm{e}^{-w(x)} + \delta_0 \, \mathrm{e}^{w_0 - w(x)}$$

where

$$w(x) = b\left[\frac{1}{x \, \mathrm{e}^x} + R(x)\right]$$

$$G(x) = a\int_{x_0}^{x} \frac{\mathrm{d}t}{t^2} \, \mathrm{e}^{w(t)}$$

and δ_0 is the initial disequilibrium.

TABLE 1

Experimental values of parameters used in the simulations

T_0	T_v	$\|q^-\| = q^+$	C_{pl}	C_{pg}
340 K	296 K	20 K min^{-1}	35.68 J mol^{-1} K^{-1}	24.42 J mol^{-1} K^{-1}

3.3 Computer simulations based on $\tau = \tau(T)$

In this section we show the computer simulations of the behavior of amorphous Se around T_g by the model just presented. In fact we analyze here the cyclic experiment (cooling–annealing–heating). Such an experiment consists in cooling the sample through the T_g range from T_0 to T_v (temperature of isothermal hold), and subsequent reheating to T_0. Table 1 is a summary of the parameters defining the experimental conditions.

At first thoughts, E and τ_0 should be adjustable parameters of the model. In practice, for the initial guess E and τ_0 were deduced, respectively, from the experimental $T_g(q^-)$ dependence and from the δ versus time fit during the isothermal stage.

Figure 3 displays the $\ln |q^-|$ versus $10^3/T_g$ observed dependence for several cooling–reheating experiments, where $|q^-| = q^+$. The value $E = 2.7$ eV/at is obtained from the slope. Notwithstanding the relative simplicity of the adopted model this value of the activation energy is in fair agreement with the one obtained ($E = 2.48$ eV/at) from viscosity measurements [20], and with the result $E = 2.1$ eV/at derived from the maxima of the AES reported in [8]. Our preliminary result for E is fairly consistent with the energy (2.1 eV/at) corresponding to the strength of a Se–Se bond in trigonal

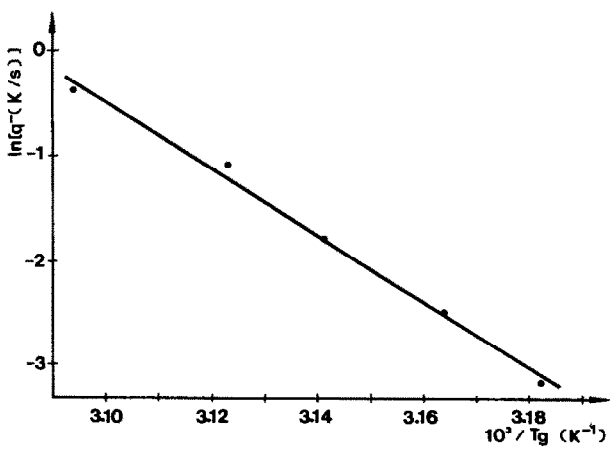

Fig. 3. Plot of $\ln |q^-|$ versus $10^3/T_g$ for several DSC measurements with different cooling–reheating rates, where $|q^-| = q^+$.

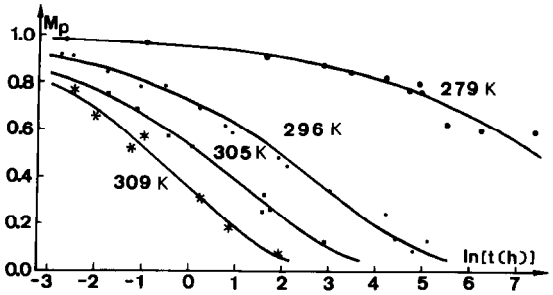

Fig. 4. Experimental time dependence of the relaxation function M_P for the relaxation of a-Se at several annealing temperatures.

chains. Therefore, this result supports the idea that a dominant role in the relaxation process of Se is played by the breaking and reconstruction of trigonal chains [21].

We now attempt to approach the value of τ_0 from the behavior during the isothermal step

$$\delta = \delta_0 \exp\left(\frac{-t}{\tau_0 \, e^{E/kT}}\right)$$

The relaxation is manifested by the change of a certain property P which is connected with δ. For the normalization of the response the following function seems to be convenient

$$M_P(t) = \frac{P_t - P_\infty}{P_0 - P_\infty} = \delta/\delta_0 = \exp\left(-\frac{t}{\tau_0 \, e^{E/kT}}\right)$$

where the subscripts to P denote the appropriate instants of time.

Figure 4 shows the experimental time dependence of M_P for several annealing temperatures when the excess enthalpy (the enthalpy relaxed during annealing and reabsorbed by the glass to reach its metastable equilibrium) was taken as the P property sensitive to the relaxation of a-Se [22]. From the slope of the straight line ln $M_P(t)$ versus t, and the previously determined value of E, we obtain an average value $\tau_0 = 5.7 \times 10^{-43}$ s. Afterwards the initial values of E and τ_0 may be iteratively modified in order to obtain the best fit to the experimental results.

Figures 5 and 6 correspond, for different cooling and heating rate ratios, to the calculated temperature plots for the fictive temperature T_f during cyclic experiments where we combine several cooling/heating rates. The cycles were performed without an isothermal hold. The outstanding features are as follows: the fictive temperature follows the actual temperature in the beginning of cooling and asymptotically approaches the constant values 324 K and 304.5 K, depending on the cooling rate. During reheating, the fictive temperature crosses the equilibrium line, and then converges with it at

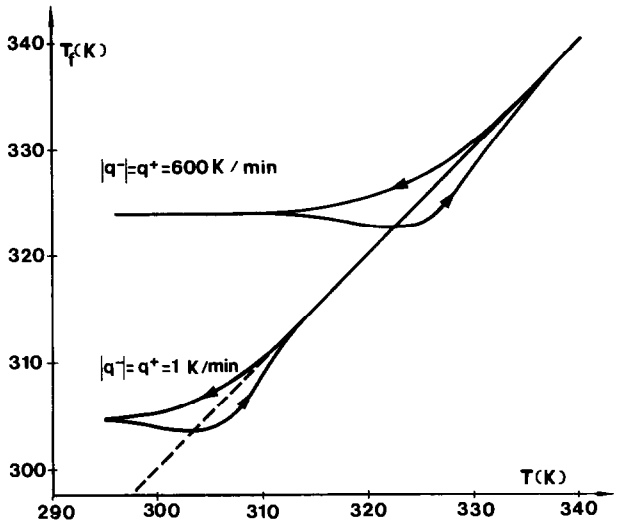

Fig. 5. Fictive temperature vs. temperature. Computer simulations of rapid–rapid and slow–slow processes based on $\tau = \tau(T)$.

higher temperatures. Slow reheating ($q^+ = 1$ K min^{-1}) provides enough time for the system to approach the equilibrium line using a short route, closely following the equilibrium line afterwards. In contrast, rapid reheating ($q^+ =$ 600 K min^{-1}) of the amorphous sample produces a large overshoot and a vigorous approach toward the equilibrium line from below.

The dependence on the time of isothermal hold at T_v is given in Fig. 7. The simulated experiments were performed with the usual parameters of

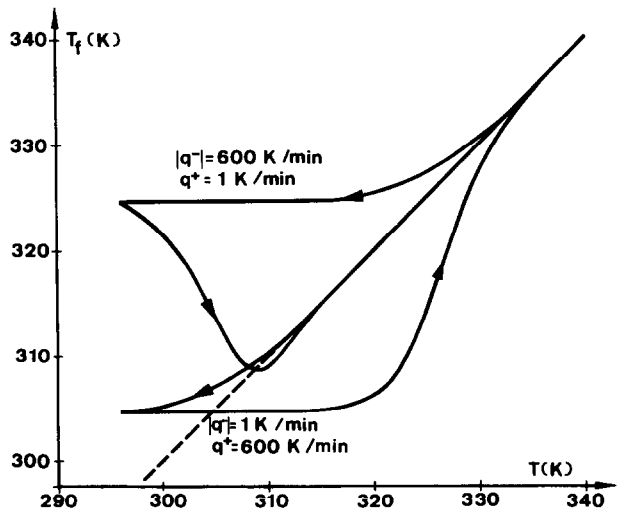

Fig. 6. Fictive temperature vs. temperature. Computer simulations of rapid–slow and slow–rapid processes based on $\tau = \tau(T)$.

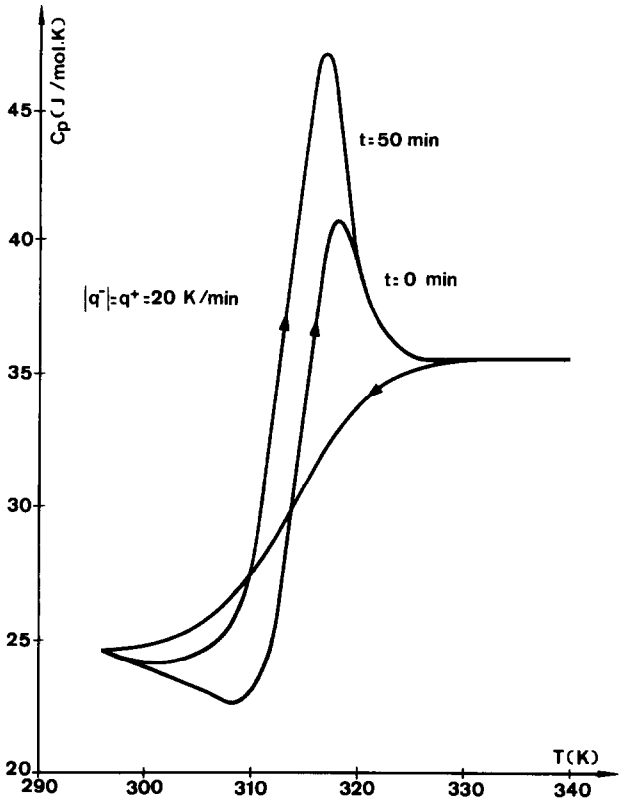

Fig. 7. Temperature dependence of the heat capacity C_p in the glass transition range. The simulated experiments were performed with the usual parameters of Table 1 and aging times of 0 and 50 min.

Table 1 and aging times of 0 and 50 min, respectively. One of the most striking features is the relaxation peak corresponding to the inflexion point of the T_f vs. T curve in the heating section. Increasing the aging time increases the area under the relaxation peak. Surprisingly, however, the temperature at the maximum decreases with the aging time; this unexpected result is in contradiction with most experimental observations, although it has been reported for B_2O_3 [2]. The usual dependence is illustrated in Fig. 8 by our own experimental results on amorphous selenium. This problem merits closer examination. The calculated evolution of the temperature at the maximum of the relaxation peak, T_{gm}, versus either $\delta(t)$ or ln t is shown in Fig. 9. It can be deduced that evolution is faster for higher annealing temperatures, although in this case the magnitude of the total shift in T_{gm} is smaller. These last conclusions are in agreement with the observed experimental results, in spite of the reversed evolution of T_{gm}.

To test the model more stringently, we analyze quantitatively the complex cyclic experiment including an isothermal hold. We now attempt to simulate

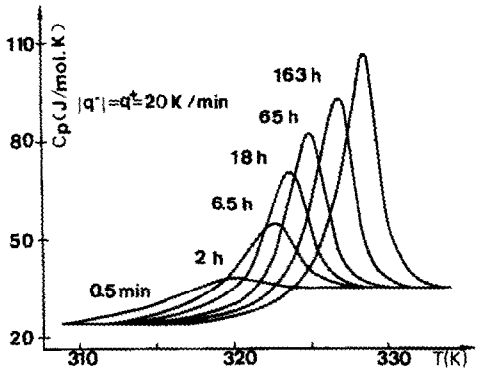

Fig. 8. Heat capacity C_p versus temperature in the region of T_g after different elapsed times at 296 K. Experimental results correspond to amorphous selenium.

the behavior of a sample of amorphous selenium annealed for 115 h at $T_v = 279$ K. The best fit was obtained with $E = 2.75$ eV/at, but the obtained result was far lower than expected. Figure 10 shows the experimental relaxation peak beside the simulated ones, and it can be seen that the height of the calculated maximum for 115 h is smaller and has an aspect ratio very different from the observed maximum. The same holds for the peak calculated with an annealing time of 720 h. In fact, we have needed to simulate an annealing time of 1248 h at 279 K in order to get a similar height.

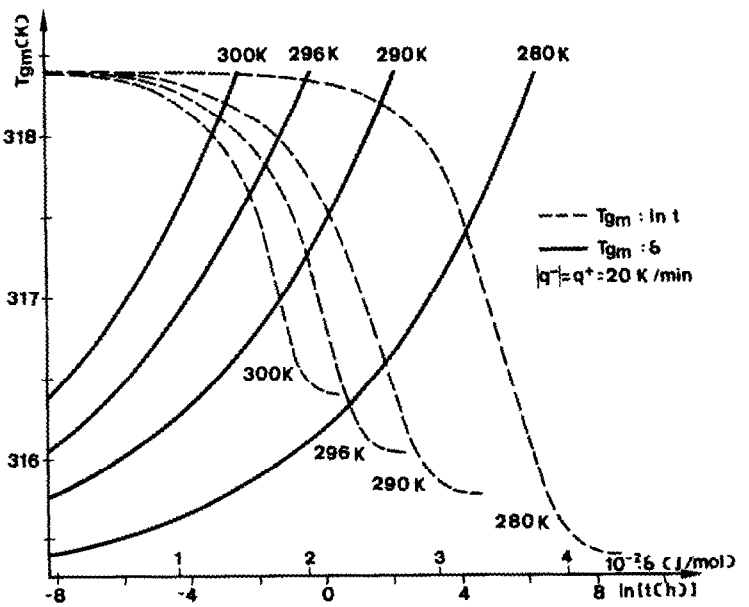

Fig. 9. Evolution of the temperature at the maximum of the relaxation peak, T_{gm}, versus either $\delta(t)$ or $\ln t$. Calculations based on $\tau = \tau(T)$.

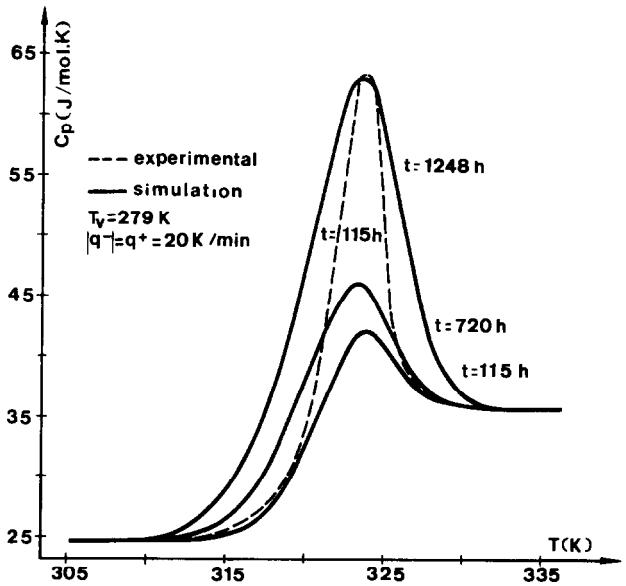

Fig. 10. Heat capacity C_p versus temperature in the region of T_g. (- - - - -) Experimental result corresponding to amorphous selenium annealed for 115 h at $T_v = 279$ K. (———) Computer simulations based on $\tau = \tau(T)$ for several annealing times.

Nevertheless, this calculated peak is broader than those observed on both sides, ascending and descending.

From the above results we conclude that this simple model, where τ accounts only for a pure thermal dependence, can yield very useful information about the main qualitative features of enthalpic relaxation. The model fails, however, to explain the sense in the shift of the relaxation peak with δ; in this respect all the $\tau = \tau(T)$ models appearing in the literature [6] fail also. Indeed, the inadequate correlation between some experimental results and the quantitative predictions of the model leads one to infer that the nonlinearity in the approach to equilibrium cannot be ruled out for these supercooled and far from equilibrium glasses.

4. COMBINED THERMAL AND STRUCTURAL DEPENDENCE

4.1 The necessity of a configuration-dependent relaxation time

Up to now we have limited ourselves to the study of the simple relaxation time $\tau = \tau(T)$. The treatment which follows concerns the general form $\tau = \tau(T, \delta)$ of the Narayanaswamy relaxation time. On inserting this relaxation time into the Kovacs relationship we obtain the equation

$$-\mathrm{d}\delta/\mathrm{d}T = \Delta C_p + \frac{1}{\tau_0 \exp(xE/kT) \exp\left[(1-x)E/k\left(T + \dfrac{\delta}{\Delta C_p}\right)\right]} \cdot \frac{\delta}{q}$$

The numerical integration of the above equation was carried out according to a method suggested by Alegria et al. [23]: calculations started with $\delta = 0$ at a high enough temperature to give $q\tau(T, 0) < 10^{-4}$. In this way the equilibrium is attained in a short time. The temperature was changed in steps ΔT and τ was fixed at the starting value during the corresponding time $t = \Delta T/q$. Values of δ at the end of the step were calculated according to

$$\delta(T + \Delta T) = \Delta C_p q\tau(T)\{\exp[-t/\tau(T)] - 1\} + \delta(T)\exp[-t/\tau(T)]$$

The last expression was obtained by analytic integration of the Kovacs equation. The new value of τ, obtained at $T + \Delta T$ together with $\delta(T + \Delta T)$, is taken as the starting value for the following step. Values of δ and τ at the low temperature end, T_v, are the starting values for the isothermal stage (during the time of conservation t_{iso}). In practice, the annealing time is subdivided in short time steps Δt in order to consider τ constant. Therefore, at the end of each interval we have

$$\delta(t + \Delta t) = \delta(t)\exp[-\Delta t/\tau(t)]$$

4.2 Simulations based on $\tau = \tau(T, \delta)$

The set of parameters and the starting values used in these simulations were the same as in the previous model, besides the partition factor $x = 0.8$ (unless we indicate to the contrary).

Figures 11 and 12 show the T_f versus T plots for the same cyclic experiment as illustrated in Figs. 5 and 6 for the first model. One can see

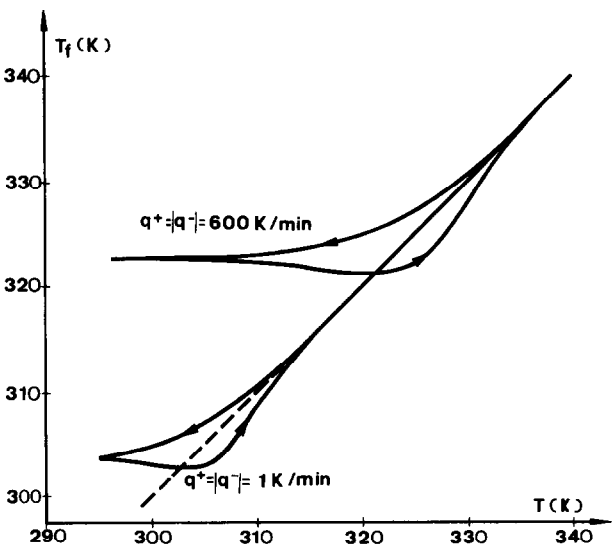

Fig. 11. Fictive temperature vs. temperature. Computer simulations of rapid–rapid and slow–slow processes based on $\tau = \tau(T, \delta)$.

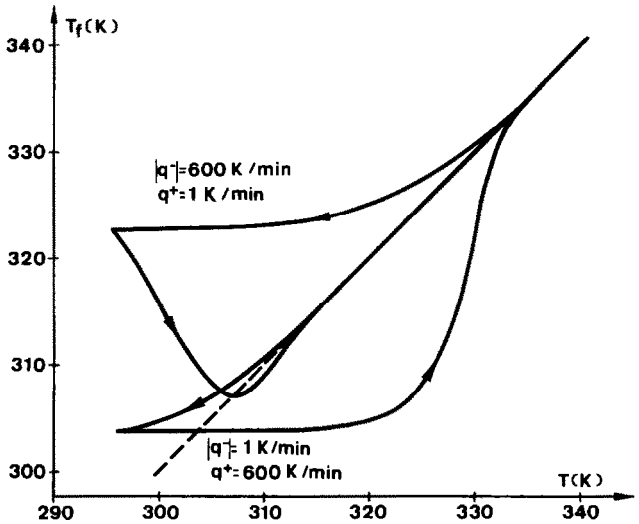

Fig. 12. Fictive temperature vs. temperature. Computer simulations of rapid–slow and slow–rapid processes based on $\tau = \tau(T, \delta)$.

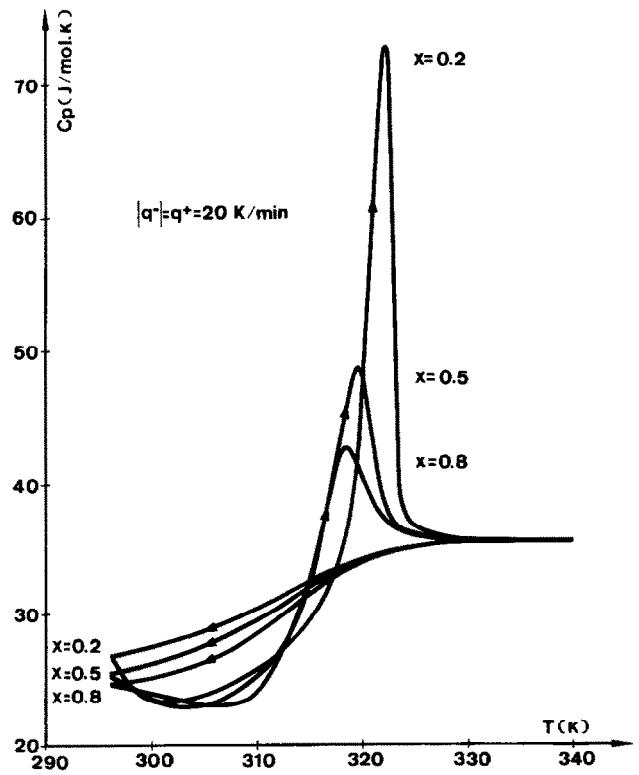

Fig. 13. Temperature dependence of the heat capacity C_p in the glass transition range. The simulated experiments were performed with the usual parameters of Table 1 and for several values of the partition parameter x. The cycles were performed without isothermal treatment.

that the qualitative results are very similar to those obtained previously, but quantitatively some differences exist.

(i) The calculated constant T_f values, corresponding to T_g, are smaller. This result indicates a larger inertia of the system to depart from equilibrium than in the $x = 1$ case.

(ii) The approach towards equilibrium when the sample is reheated is faster than in the previous case (i.e., the magnitude of the overshoot is greater).

These observations seem to indicate the increasing importance of the apparent forces which equilibrate the system as x decreases.

Figure 13 illustrates the changes produced in the relaxation peak when the partition parameter x is modified about some values. Sharper peaks are seen to be characteristic of smaller values of x, corresponding to larger nonlinearities (i.e., a stronger dependence with the structure).

It is interesting to study the shift of the relaxation peaks with the annealing time or the departure from equilibrium, δ. Figure 14 shows that for $x = 0.8$ all the cyclic experiments give an initial stage of reversed evolution beyond which the shift fits the real behavior. Nevertheless, for $x = 0.5$ the shift is correct during the entire experiment. We think that this is

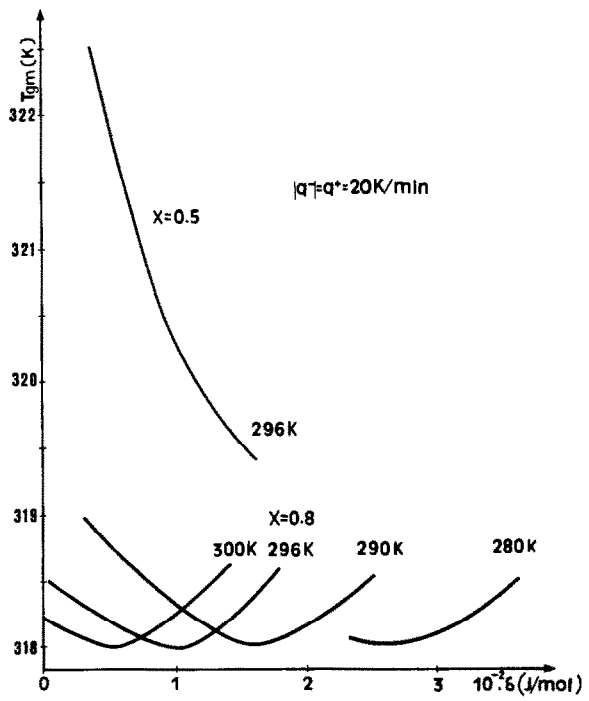

Fig. 14. Evolution of the temperature at the maximum of the relaxation peak, T_{gm}, versus $\delta(t)$. Computer calculations based on $\tau = \tau(T, \delta)$ for several annealing temperatures and different values of the partition parameter x.

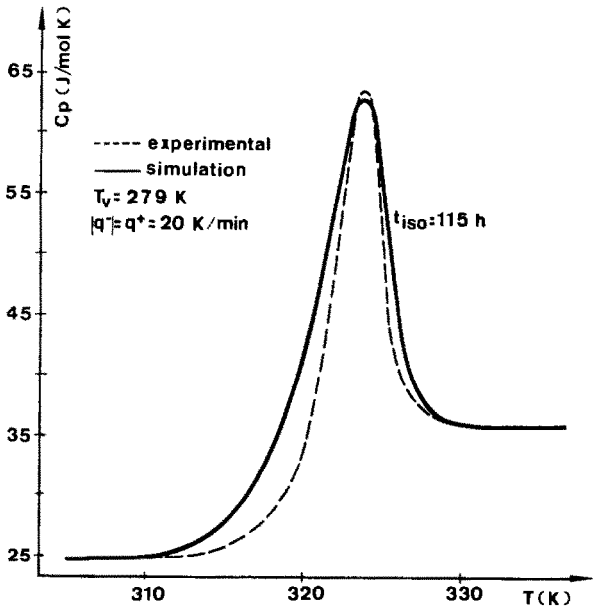

Fig. 15. Heat capacity C_p versus temperature in the region of T_g for an annealing time of 115 h at $T_v = 279$ K. (- - - - - -) Experimental result for amorphous selenium. (———) Computer simulation based on $\tau = \tau(T, \delta)$.

an important result which allows us to attribute the observed direction of the shift to nonlinear effects during the approach to equilibrium.

Finally, Fig. 15 displays the same simulation of the full cyclic experiment with $t_{iso} = 115$ h and $T_v = 279$ K which was referred to in Fig. 10. A reasonable agreement was found for $E = 2.7$ eV/ at and $x = 0.75$. The key appears to lie in the mentioned ability of the model allowing for sharper peaks than for the $x = 1$ model.

5. CONCLUSIONS

Many features of the glass transition phenomena may be described satisfactorily in terms of the phenomenological model of Kovacs including the Narayanaswamy relaxation time. When this approach is applied to samples of amorphous Se, the enthalpy relaxation can be interpreted by means of kinetic parameters such as relaxation times or apparent activation energies. If we adopt the value $x = 1$ for the partition factor in $\tau(T, \delta)$, we are concerned with the pure thermal dependence model, $\tau = \tau(T)$. The preliminary analysis of this model allows us to emphasize some theoretical aspects which are not likely to be recognized in more complex models. The model calculations demonstrate that the temperature location and height of the enthalpy relaxation peak are closely related to the activation energy E

and the partition factor x, respectively. The simulations of the shift of the relaxation maximum with δ show the importance of the structural contribution to the relaxation time in real processes.

However, the use of a single relaxation time can give only an approximate account of a complex relaxation, particularly in the glassy state. The most severe limitation consists in the inadequacy to describe the memory effects currently observed around T_g. Further work, allowing for a deeper insight into enthalpy relaxation, is afforded by considering a distribution of relaxation times, and will be reported as a continuation to this paper.

REFERENCES

1 O.S. Narayanaswamy, J. Am. Ceram. Soc., 54 (1971) 491.
2 M.A. Debolt, A.J. Easteal, P.B. Macedo and C.T. Moynihan, J. Am. Ceram. Soc., 59 (1976) 16.
3 J.M. O'Reilly, J. Appl. Phys., 50 (1979) 6083.
4 H.S. Chen and T.T. Wang, J. Appl. Phys., 52 (1981) 5893.
5 A.J. Kovacs, J.J. Aklonis, J.M. Hutchinson and A.R. Ramos, J. Polym. Sci., 17 (1979) 1097.
6 A.J. Kovacs, J.M. Hutchinson and J.J. Aklonis, in P.H. Gaskell (Ed.), Structure of Non-Crystalline Materials, Taylor & Francis, London, 1977, p. 153.
7 A. Muñoz, F.L. Cumbrera and R. Marquez, Current Topics on Non-Crystalline Solids, World Scientific Co., Philadelphia, PA, 1986, p. 211.
8 A. Muñoz, F.L. Cumbrera and R. Marquez, Mater. Chem. Phys., 21 (1989) 279.
9 R.B. Stephens, J. Appl. Phys., 49 (1978) 5855.
10 A.R. Cooper, J. Non-Cryst. Solids, 71 (1985) 5.
11 T.S. Chow, J. Non-Cryst. Solids, 75 (1985) 209.
12 J.R. Cost, J. Appl. Phys., 54 (1983) 2137.
13 F. Twyman, J. Soc. Glass. Technol., 1 (1917) 61.
14 O.S. Narayanaswamy, J. Am. Ceram. Soc., 54 (1971) 491.
15 T.S. Chow and W.M. Prest, J. Appl. Phys., 53 (1982) 6568.
16 A.Q. Tool, J. Am. Ceram. Soc., 29 (1946) 240.
17 J.M. Hutchinson and A.J. Kovacs, in P.H. Gaskell (Ed.), Structure of Non-Crystalline Materials, Taylor & Francis, London, 1977, p. 167.
18 Handbook of Mathematical Functions, by M. Abramowitz and I.A. Stegun (Eds.), National Bureau of Standards, Applied Mathematics Series, U.S. Dept. of Commerce, Washington, 1965.
19 C.T. Moynihan, J. Wilder and J. Tucker, J. Phys. Chem., 78 (1974) 2673.
20 M. Matsuura and K. Suzuki, J. Mater. Sci., 14 (1979) 395.
21 J.P. Larmagnac, J. Grenet and P. Michon, J. Non-Cryst. Solids, 45 (1981) 157.
22 S. Suriñach, N. Clavaguera and M.D. Baro, Mater. Sci. Eng., 97 (1988) 533.
23 A. Alegria, J.M. Barandiaran and J. Comenero, Phys. Status Solidi B, 120 (1983) 349.